A Method for Assessing the Stability of a Membrane Protein†

Francis W. Lau and James U. Bowie*

Department of Chemistry and Biochemistry and Laboratory of Structural Biology and Molecular Medicine, University of California at Los Angeles, 405 Hilgard Avenue, Los Angeles, California 90095-1570

Received December 17, 1996; Revised Manuscript Received March 6, 1997⊗

ABSTRACT: The integral membrane protein diacylglycerol kinase (DGK) from *Escherichia coli* has been reversibly unfolded in a protein/detergent/mixed micelle system by varying the molar ratio of *n*-decyl β-D-maltoside (DM) and sodium dodecyl sulfate (SDS). Unfolding was monitored by circular dichroism (CD) and ultraviolet (UV) absorbance spectroscopy. When unfolding is monitored by measuring changes in absorbance at 294 nm, two distinct denaturation phases are observed, indicative of a stable intermediate. When CD is used as a conformational probe, the resulting denaturation curve contains only one major transition, which corresponds to the first unfolding phase observed by absorbance changes. The unfolding behavior of several mutant proteins in which the tryptophan residues were selectively replaced made it possible to assign the first unfolding phase to a denaturation event in a cytoplasmic domain and the second phase to denaturation of the membrane-embedded portion of the protein. The denaturation curves fit well to a model which assumes two cooperative transitions and a linear relationship between unfolding free energy and SDS concentration. Extrapolation back to zero denaturant indicates an unfolding free energy of 6 kcal/mol for the cytoplasmic domain and 16 kcal/mol for the transmembrane domain. The high apparent stability of the transmembrane domain could explain the high degree of tolerance to amino acid substitutions seen for DGK and other membrane proteins. The approach described in this paper may be applicable to other membrane protein systems.

Diacylglycerol kinase from *Escherichia coli* (DGK)[1] is a small integral membrane protein, consisting of only 121 amino acids (Lightner et al., 1983; Loomis et al., 1985). DGK catalyzes the transfer of the γ-phosphate of ATP to diacylglycerol, producing phosphatidic acid and ADP. The topology, defined by β-lactamase and β-galactosidase fusion experiments, consists of two cytoplasmic α-helices (approximately residues 1−34 and 69−95) and three transmembrane domains (approximately residues 35−48, 52−68, and 96−117) (Smith et al., 1994) (see Figure 1). Recent cross-linking results indicate that the folded protein is trimeric (C. Sanders, personal communication). Although the enzymatic activity of the protein has been well characterized (Loomis et al., 1985; Walsh & Bell, 1986a,b; Walsh et al., 1990; Sanders, et al., 1996), methods for evaluating thermodynamic stability have not been described. We recently completed a large study of the tolerance of DGK to amino acid substitutions (Wen et al., 1996). Every residue in the protein was mutagenized, and substitutions that allow protein function were identified. Most of the critical (invariant) residues were found to reside in the second cytoplasmic domain, and this region probably constitutes much of the active site. One of the hallmarks of the mutagenesis study was the high level of substitution tolerance permitted throughout most of the DGK sequence, particularly in the transmembrane domains. The results of this paper offer a possible explanation of how such tolerance is accommodated.

Compared to water-soluble proteins, there is a dearth of experimental information regarding the folding and thermodynamic stability of membrane proteins. Current knowledge concerning the stability of membrane proteins has been derived primarily from thermal denaturation studies on bacteriorhodopsin (Brouillette et al., 1987, 1989; Kahn et al., 1992), erythrocyte band 3 (Davio & Low, 1982; Maneri & Low, 1988), cytochrome *c* oxidase (Rigell et al., 1985; Morin et al., 1990), and photosystem II (Cramer et al., 1981; Thompson et al., 1986, 1989). In each of these systems, thermal denaturation leads to an irreversibly denatured state, complicating the interpretation of the results. Thermal denaturation of DGK solubilized in detergent micelles also results in irreversible aggregation (unpublished). Unlike soluble proteins, denaturants have been used in only a few cases to study the thermodynamics or kinetics of membrane protein folding (Oikawa et al., 1985; Hill et al., 1988; Booth et al., 1995; Klug et al., 1995). Nevertheless, it is clear from a number of studies that many membrane proteins can be refolded after denaturation with chemical denaturants such as guanidine hydrochloride (GuHCl), urea, or SDS (Huang et al., 1981; London & Khorana, 1982; Dornmair et al., 1990; Eisle & Rosenbusch, 1990; Klug et al., 1995). In the case of DGK, it has been shown that activity can be recovered after denaturation by urea and acidic organic solvents (Bohnenberger & Sandermann, 1979; Loomis et al., 1985; Sanders et al., 1996), suggesting that it might be possible to

† This work was supported by grants from the DOE, the NSF, and the Pew charitable trusts.

* Author to whom correspondence should be addressed. Telephone: (310) 206-4747. Fax: (310) 206-4749. E-mail: bowie@ewald.mbi.ucla.edu.

⊗ Abstract published in *Advance ACS Abstracts,* April 15, 1997.

[1] Abbreviations: ADP, adenosine diphosphate; ATP, adenosine triphosphate; CD, circular dichroism; DAG, 1,2-*n*-dioleoylglycerol; DGK, diacylglycerol kinase; DM, *n*-decyl β-D-maltoside; GuHCl, guanidine hydrochloride; IPTG, isopropyl-β-D-galactosidase; LB, Luria-Burtani; LDH, lactate dehydrogenase; NADH, nicotinamide adenine dinucleotide (reduced form); NAD^+, nicotinamide adenine dinucleotide (oxidized form); OG, *n*-octyl β-D-glucoside; PCR, polymerase chain reaction; PK, pyruvate kinase; SDS, sodium dodecyl sulfate; PMSF, phenylmethanesulfonyl flouride; UV, ultraviolet; buffer A, 50 mM sodium phosphate and 0.30 M NaCl at pH 7.5.

S0006-2960(96)03095-4 CCC: $14.00

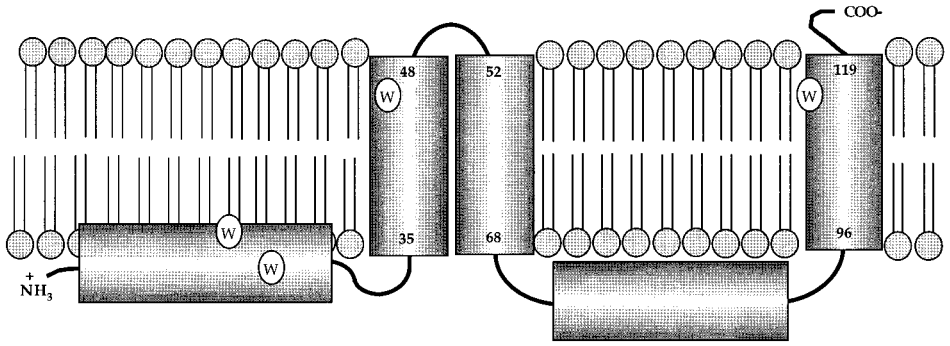

FIGURE 1: Topological model of DGK. The topology of DGK derived from the β-lactamase and β-galactosidase fusion experiment of Smith et al. (1994) is shown. DGK is predicted to consist of two cytoplasmic helices ($\sim$1−34 and $\sim$69−95) and three transmembrane-spanning segments ($\sim$35−48, $\sim$52−68, and $\sim$96−117) which are also depicted as α-helices. The approximate positions of the tryptophan residues are also shown.

develop a system with which to observe reversible folding of DGK.

In this study, we have used SDS as a denaturant. The ability of SDS to denature proteins is well-established, and we believe SDS has several advantages over GuHCl and urea, the denaturants traditionally used for soluble proteins. Unlike GuHCl and urea, SDS is capable of forming mixed micelles with other detergents. As a result, a lipid-like environment can be maintained for the membrane-embedded portions of the protein and complexities associated with detergent removal from protein are avoided. Furthermore, α-helical content is frequently preserved in SDS (Reynolds & Tanford, 1970; Mattice et al., 1976). The unraveling of α-helices in a membrane bilayer is extremely unfavorable (Engelman et al., 1986; Popot & Engelman, 1990; Zhang et al., 1992; Deber et al., 1993). Therefore, a denatured state which retains most of the native helical structure is likely to be a more relevant model for the unfolded protein within a membrane than the random coil state induced by GuHCl and urea (Popot & Engelman, 1990). Indeed, both thermally denatured bacteriorhodopsin and cytochrome *c* oxidase appear to retain much of their native helical content (Brouillette et al., 1987; Kahn et al., 1992; Arrondo et al., 1994). Here we show that DGK is reversibly unfolded by SDS and retains much of its helical content. Our results suggest that the transmembrane domain structure is very stable and is substantially more stable than the domain outside the membrane.

MATERIALS AND METHODS

Materials. Sodium dodecyl sulfate (SDS), approximately 99% (GC), Pipes, and NADH were all purchased from Sigma. Dioleoylglycerol (DAG) and cardiolipin were from Avanti Polar Lipids (Birmingham, AL). The nonionic detergents *n*-octyl β-D-glucoside (OG) and *n*-decyl β-D-maltoside (DM) were obtained from either Calbiochem or Anatrace. Ni−NTA−agarose resin was obtained from Qiagen, Inc. (Chatsworth, CA).

Synthetic Gene. Plasmids pSD003 and pSD004, containing a synthetic gene that codes for the DGK enzyme, were constructed. The synthetic gene plasmids are derivatives of pTrcHisB (Invitrogen), and the genes are expressed from the strong isopropyl-β-D-galactosidase (IPTG) inducible promoter, P*trc*. The encoded proteins incorporate N-terminal leader sequences containing a His_6 sequence used in purification (see below). The two synthetic genes differ in the length of the N-terminal leader sequence. The N-terminal leader sequence encoded by pSD003 can be removed by enterokinase digestion, while the short leader of pSD004 cannot. After much of the work in this paper was completed, we discovered that, due to typographical errors while designing the gene, the sequences encoded by the synthetic gene plasmids differed from the natural *E. coli* sequence at two positions. The synthetic genes encode an Arg at position 117 rather than a Trp and a Thr at position 118 rather than a Ser. However, as judged by enzyme kinetic parameters and SDS unfolding experiments, the enzymes encoded by the synthetic genes are indistinguishable from the one encoded by the wild-type sequence. To differentiate between our enzymes and the natural enzyme, we call the proteins encoded by pSD003 and pSD004 as SynDGK-3 and SynDGK-4. All experiments in this paper were performed with the SynDGK-4 enzyme, and we will refer to this sequence as the wild-type sequence throughout the paper.

The synthetic DGK gene was built up *in vitro* using a series of polymerase chain reaction (PCR) steps. Seven oligonucleotides about 80 bases in length were synthesized, which encompassed the entire bottom strand of the gene shown in Figure 2, through the *Sac*I site at the 5′ end and the *Hin*dIII site at the 3′ end. The synthesized DNA extended 12 base pairs past the *Sac*I site at the 5′ end and 12 base pairs past the *Hin*dIII site at the 3′ end of the gene to facilitate subsequent restriction enzyme digestion. Each oligonucleotide contained an 18-base overlap with its neighbor in the sequence. A 22-base top strand primer was also prepared at the extreme 5′ end of the synthetic DNA sequence for PCR amplification. Seven PCR steps were performed to build up the gene from the 5′ end using standard conditions with Taq polymerase. The size of the PCR product was verified at each step. The final DNA product was digested with *Sac*I and *Hin*dIII and ligated with *Sac*I- and *Hin*dIII-digested pTrcHisB (Invitrogen). A number of clones were sequenced, and all contained multiple mutations. Mutations were repaired by replacing segments with either synthetic cassettes or regions from other clones that were known to have the correct sequence, to yield plasmid pSD003. The sequence of the entire gene was verified by sequencing both strands. A second plasmid, pSD004, was prepared containing a shortened N-terminal tail sequence by replacing the 5′ leader sequence of pSD003 with a synthetic oligonucleotide cassette.

Construction of Mutants. Genes encoding W47F and W112F were prepared by replacing the wild-type sequence with synthetic DNA cassettes encoding the mutations. For

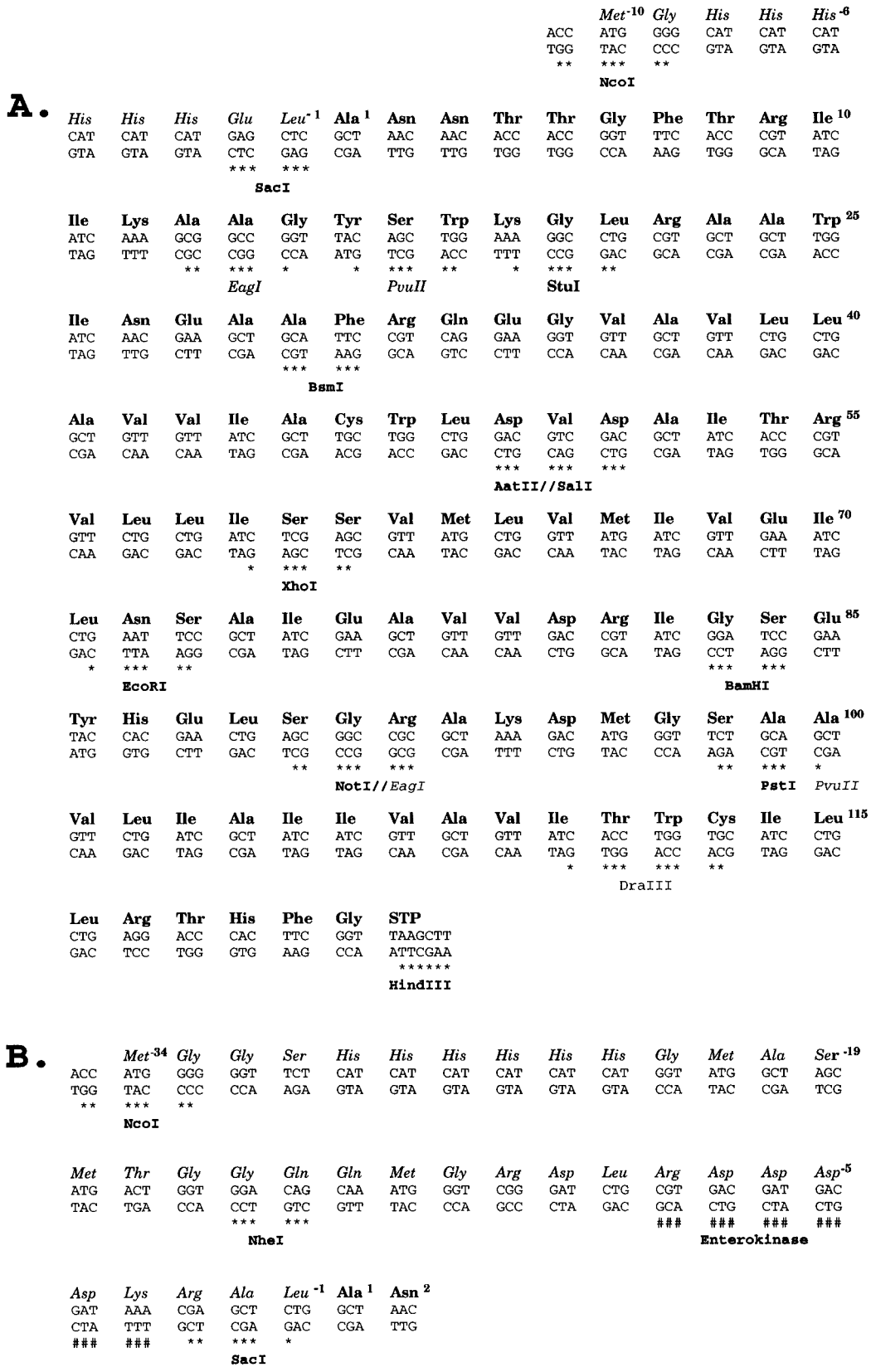

FIGURE 2: The synthetic DGK genes. (A) The synthetic DGK gene sequence in pSD004. (B) The leader sequence of pSD003. The restriction sites shown in bold are unique in the plasmid. The leader amino acid sequence is shown in italics, and the amino acid sequence of the wild-type *E. coli* enzyme is shown in bold. Position 1 corresponds to the N-terminal amino acid of the natural enzyme after cleavage of the first methionine residue (Loomis et al., 1985).

W47F, the region between the *Bsm*I and *Sal*I sites was replaced, and for W112F, the region between the *Pst*I and *Hin*dIII sites was replaced. As the codon for leucine differs from the codon for tryptophan by a single base, it was possible to construct genes encoding the mutant proteins W18L, W25L, and W18L/W25L in a single cloning step. The region from *Sac*I to *Bsm*I of pSD004 was replaced with a synthetic DNA cassette in which the second position of both tryptophan codons was synthesized with an equal mixture of G and T on the top strand and an equal mixture

of C and A on the bottom strand. In all cases, the mutations were identified by sequencing the entire replaced region.

Purification. Plasmids expressing the DGK variant to be purified were introduced into *E. coli* strain WH1061 in which the chromosomal DGK gene was disrupted (Miller et al., 1992). LB media containing 100 μg/mL ampicillin was inoculated with an overnight culture grown in the same media. The culture was incubated at 37 °C until the absorbance at 600 nm reached 1.0 in a 1 cm cuvette. DGK expression was then induced by adding IPTG to a final concentration of 200 μg/mL. After incubation for an additional 4 h, the cells were harvested by centrifugation and stored frozen at −80 °C.

All purification steps were carried out at 4 °C. In a standard purification, 12 g of frozen cells was resuspended in 120 mL of buffer A (50 mM sodium phosphate and 0.30 M NaCl at pH 7.5) containing 1 mM PMSF. Octyl β-D-glucopyranoside (OG) was added to a final concentration of 3% (w/v) and the suspension stirred for 2 h to solubilize DGK. Insoluble material was then removed by centrifugation in a Sorvall SS-34 rotor at 15 000 rpm for 30 min. The supernatant was mixed with 12 mL (bed volume) of Ni−NTA−agarose (Qiagen) resin which had been previously equilibrated in buffer A and agitated gently for 2 h. The resin with bound protein was then pelleted by centrifugation in a Sorvall GSA rotor at 5000 rpm for 5 min and the supernatant discarded. The resin was then resuspended in 120 mL of buffer A containing 1.5% OG and 0.03 M imidazole (imidazole was added from a 2 M stock solution adjusted to pH 8.0). The resin was collected again by centrifugation, resuspended in a small volume of buffer A containing 1.5% OG and 0.03 M imidazole, and packed in a small column. The column was washed in the same buffer until the absorbance of the effluent at 280 nm dropped to less than 0.1 (typically 10−15 column volumes). At this point, the detergent was changed to DM by washing with five column volumes of buffer A containing 0.5% DM without any imidazole (the affinity of the protein for the Ni−NTA resin is significantly reduced in DM so it would be washed off even in low imidazole). The protein was then eluted in buffer A containing 0.5% DM and 0.25 M imidazole. The typical yield of purified protein is in the range of 60−85 mg of enzyme from 12 g of wet cell paste (about 4 L of culture). The eluted protein can be stored at −80 °C after flash freezing either with liquid nitrogen or with a dry ice/ethanol bath. Full activity is recovered upon thawing of frozen aliquots.

Protein Concentration. Protein concentration was determined by absorbance at 280 nm, using extinction coefficients of 25 200 M^{-1} cm^{-1} for the wild-type protein and 19 600 M^{-1} cm^{-1} for both W47F and W112F. For the double mutant W18L/W25L, the extinction coefficient was 14 000 M^{-1} cm^{-1}. These values were calculated on the basis of the number of tyrosine and tryptophan residues according to the method described by Copeland (1994).

Activity Assay. DGK activity was measured using a coupled enzyme assay system based on the one developed by Sanders and co-workers (C. Sanders, personal communication). The production of ADP from the DGK-catalyzed reaction was detected in a two-step process. In the first step, the generated ADP and phosphoenolpyruvate, present in the assay mix, were converted to ATP and pyruvate by the action of pyruvate kinase (PK). In the second step, pyruvate was reduced to lactate by the action of lactate dehydrogenase (LDH), converting NADH to NAD^+. The oxidation of NADH could be conveniently monitored at 340 nm. Concentrations of the various components were adjusted so that the DGK-catalyzed reaction was rate-limiting. The composition of the standard assay mix was as follows: 1.0 mM phosphoenolpyruvate, 2.5 mM NADH, 14 units of PK, 22 units of LDH, 5 mM MgATP, 15 mM $MgCl_2$, 7.0 mol % 1,2-*sn*-dioleoylglycerol, 3.5 mol % cardiolipin, and 1.5% (w/v) OG. The components were dissolved in 60 mM Pipes buffer at pH 6.85. The assay mix (1.0 mL) was prepared in a 1 cm path length cuvette and preincubated until the residual ADP was consumed (i.e. until no further drop in absorbance at 340 nm was detected, typically 5 min). The reaction was then initiated by the addition of 5−10 μL the enzyme preparation.

DM Assay. Because DM concentrations were an important variable in the unfolding reactions, it was important to determine DM concentrations in every protein preparation. A modified version of the phenol−sulfuric acid reaction, first described by Dubois et al. (1956) for the quantitative determination of sugars, was employed to measure DM concentrations. Ten microliter samples were mixed with 1.0 mL of 1.0% (w/v) phenol in concentrated H_2SO_4 and warmed for 2 h at 45 °C. Samples were then cooled on ice, and their absorbance at 490 nm was read. A linear relationship between absorbance and DM concentration is seen within the range of 0.5−3.5% (w/v) DM. Samples were compared to standards to determine the DM concentration.

Spectroscopy. CD measurements were taken using an AVIV model 62DS circular dichroism spectrometer. Spectra were recorded using a 0.1 mm path length cell at a protein concentration of 0.57 mg/mL. Denaturation experiments monitored by CD were performed in appropriate path length cells to maintain the absorbance below 1.0 at 222 nm. UV measurements were performed on a Shimadzu UV-160A double-beam spectrometer, and cell path lengths were chosen to obtain absorbance values of approximately 0.5−1.0 at 294 nm.

Denaturation Procedure. Denaturation experiments were typically performed in the following manner. DGK samples in 10 mM Pipes, 0.30 M NaCl (pH 7.0), and 1.0% (w/v) DM were titrated with aliquots of 15% (w/v) SDS in 10 mM Pipes and 0.30 M NaCl at pH 7.0. Absorbance and ellipticity measurements were corrected to account for the changes in volume. All experiments were performed at room temperature. Mole fractions were calculated using the total detergent concentration rather than some estimate of the concentration in micelles, because it is not clear how much SDS remains free in this system. Relevant alterations to these basic conditions are described where appropriate below.

For the wild-type CD and UV denaturation curves, a linear baseline could be obtained for the unfolded state when data were plotted as a function of bulk SDS concentration rather than as a function of mole fraction. Folded state baseline estimations could not be made, however, due to substantial curvature in this region of the plot. Therefore, in all but one case, unfolding curves were simply normalized according to

$$f = (Y - Y_{min})/(Y_{max} - Y_{min}) \quad (1)$$

in which f denotes the fractional change, Y denotes the signal

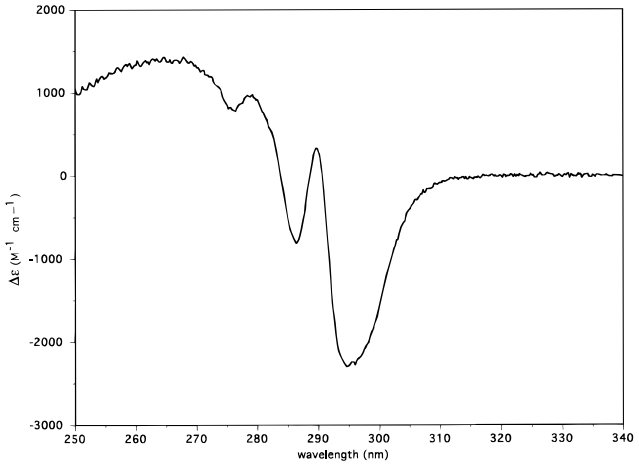

FIGURE 3: UV absorbance difference between native and denatured DGK. For the native protein, the spectrum of a 25 μM sample of DGK in 1.0% DM, 100 mM Pipes, and 0.30 M NaCl at pH 7.0 was recorded after subtraction of a buffer blank. For denatured DGK, a 25 μM sample in 15% SDS, 10 mM Pipes, and 0.30 M NaCl at pH 7.0 was recorded in a similar manner. The difference plot was constructed by subtraction of the native spectrum from the denatured one.

from either absorbance or CD, and Y_{min} and Y_{max} are the minimum and maximum values, respectively, for a given set of data. In the case of W18L/W25L, however, suitable baselines for both the folded and unfolded states could be obtained from the UV data. Therefore, in this one case it was possible to correct for the baselines by making Y_{min} and Y_{max} in eq 1 linearly dependent on the SDS concentration.

RESULTS

Spectroscopic Probes of Unfolding. The near-UV absorbance spectrum of DGK is dominated by its four tryptophan residues, and complete denaturation by SDS produces a characteristic difference spectrum (Figure 3) similar to ones observed for SDS denaturation of soluble proteins (Rao & Prakash, 1993; He et al., 1995). The difference spectrum shows two negative peaks at 286 and 294 nm which correspond to changes in absorbtivity of approximately 4 and 15%, respectively. In contrast, the absorbance of free tryptophan is significantly enhanced in SDS relative to DM, resulting in positive rather than negative peaks in the same region. Thus, the changes observed at 294 nm are most likely the result of conformational transitions rather than the result of the solvent perturbation effects of SDS.

Circular dichroism was also employed to study the unfolding of DGK by SDS. The CD spectra of native and SDS-denatured DGK are shown in Figure 4. The overall shape of the CD spectrum is consistent with the high helical content of 74% estimated from the FTIR spectrum (Sanders et al., 1996). We attempted to estimate the helical content using the methods of both Yang et al. (1986) and Manavalan and Johnston (1987) but were unable to obtain acceptable fits, suggesting that the set of basis spectra derived from soluble proteins may be inappropriate in this case. The spectrum in SDS shows a slight but significant reduction in magnitude. At 222 nm, the magnitude of the ellipticity drops 15% in SDS, which is large enough to be a useful probe of unfolding. Even after complete denaturation by SDS, however, much of the helical content appears to be retained (Figure 4).

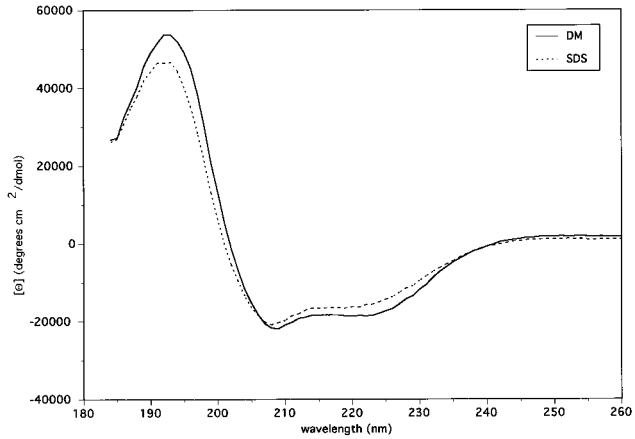

FIGURE 4: Circular dichroism spectra of DGK in DM and SDS. The samples contained 0.57 mg/mL DGK in 10 mM Pipes at pH 7.0 and either 1.0% DM (—) or 0.5% DM/10% SDS (- - -). A cell path length of 0.1 mm was used. Data were collected for every 1 nm with a 1 s acquisition time at each wavelength. The spectra are an average of 20 repetitions.

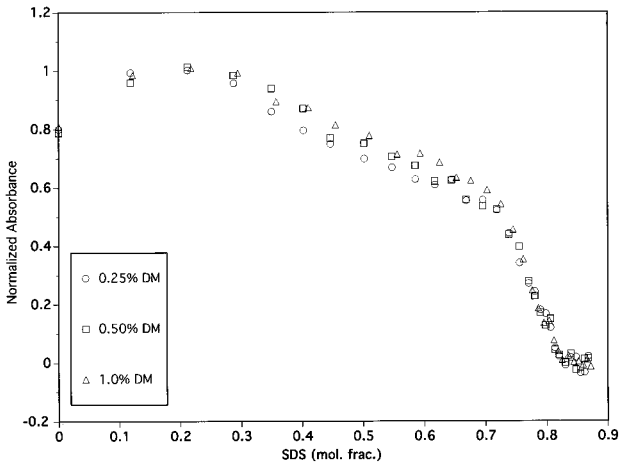

FIGURE 5: Denaturation of DGK monitored by absorbance at 294 nm. DGK in a range of starting concentrations of DM was unfolded by additions of SDS, and denaturation of DGK was monitored by absorbance at 294 nm. Absorbance values were normalized to range from 0 to 1 as described in Materials and Methods. Unfolding occurs at similar concentrations of SDS when data are plotted as a function of the mole fraction of SDS. If plotted as a function of the total concentration of SDS, the midpoints of the transitions do not coincide and are proportional to the starting DM concentrations. The initial conditions were 22 μM DGK in 10 mM Pipes (pH 7.0), 0.30 M NaCl, and (○) 0.25% DM, (□) 0.5% DM, and (△) 1.0% DM.

A dramatic reduction (30%) in fluorescence intensity at 330 nm was observed upon SDS denaturation of DGK (not shown). Essentially the same drop in fluorescence intensity was seen with free tryptophan. As a result, we could not distinguish between intensity changes due to environmental alterations and those due to conformational transitions.

Unfolding Monitored by Absorbance. As shown in Figure 5, complex changes were observed in absorbance at 294 nm as a function of SDS concentration. An initial enhancement was followed by a biphasic drop in absorbance. In contrast, free tryptophan in a DM solution shows an increase that is roughly linear in bulk SDS concentration over the same range (not shown). This initial enhancement most likely reflects a conformational change in the folded state since DGK is known to be activated by low concentrations of SDS (Walsh & Bell, 1986b). Moreover, an analogous enhancement in helical content is observed by CD.

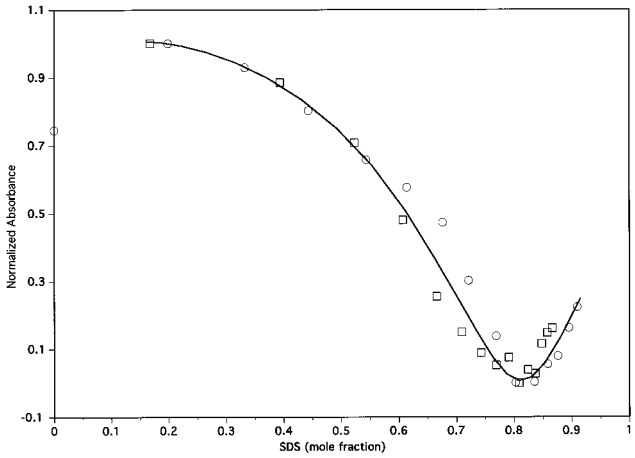

FIGURE 6: Reversibility of denaturation by SDS. Samples of DGK in excess SDS were refolded by addition of varyious amounts of DM. Each absorbance measurement was made at final DGK concentrations of 25 μM (□). For comparison, the change in absorbance at 294 nm of a DGK sample (initial concentrations of protein and detergent were 25 μM and 1.0%, respectively) was monitored as a function of the amount of SDS added (○). Absorbance values were normalized to range from 0 to 1 for each set of data as described in Materials and Methods.

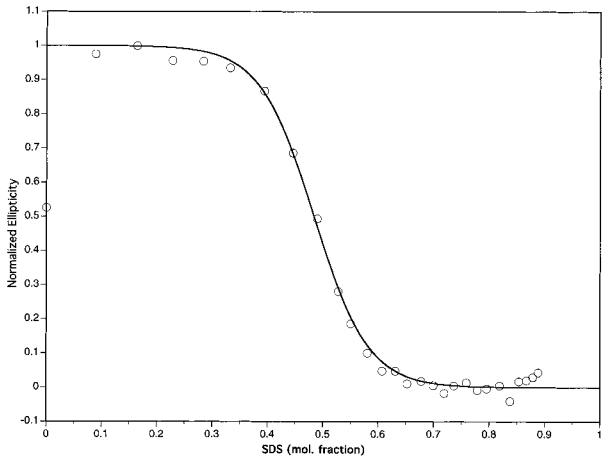

FIGURE 7: DGK unfolding monitored by CD. DGK (1.8 μM) in 10 mM Pipes (pH 7.0), 100 mM NaCl, and 1.0% DM was denatured by additions of 15% SDS in 10 mM Pipes at pH 7.0. Ellipticity measurements were made at 222 nm with a band width of 2.0 nm. Each data point represents the average value within a 30 s time interval. Ellipticity values were normalized to range from 0 to 1 as described in Materials and Methods. The curve is a fit to a two-state model as described in the text.

To demonstrate that the unfolding phenomenon occurs within the micelle environment, the effect of varying concentrations of DM was tested. As shown in Figure 5, the data exhibit surface dilution effects characteristic of mixed micelle systems. When the data are plotted in terms of either the mole ratio or the mole fraction of SDS, the different DM concentrations produced the same denaturation curve. When the data are plotted in terms of bulk SDS concentration, however, the position of the unfolding phases was shifted in proportion to the DM concentration.

Equilibrium Conditions. The unfolding reaction appears to be at equilibrium throughout the transition zones. First of all, 90% of the enzymatic activity can be recovered by dilution of the SDS-denatured DGK into a DM solution (data not shown). Second, if additions of SDS are halted at points throughout the transition, the absorbance remains stable for 30 min time periods. Third, as is shown in Figure 6, the overall process is reversible. When SDS-denatured DGK is the starting point, addition of DM causes an increase in absorbance which coincides with the transition observed when starting from a fully native protein and adding SDS.

Circular Dichroism. When the unfolding reaction is monitored by ellipticity at 222 nm, the curve is significantly different than the one seen by absorbance changes. As shown in Figure 7, an initial enhancement is observed, similar to the one seen by absorbance, but only a single denaturation phase is apparent. The ellipticity changes appear to correspond to the initial enhancement and first denaturation phases seen by absorbance, although more complex interpretations are possible. The second phase, seen by absorbance changes, is not detected by these circular dichroism measurements, as no further decrease in ellipticity at 222 nm is observed at the higher SDS concentrations. Thus, the drop in helical content occurs almost entirely within the first phase. As with the absorbance transitions, the conformational changes observed by CD appear to be dependent on the mole fraction of SDS rather than on bulk concentrations since identical denaturation curves were obtained with different initial DM concentrations (not shown).

Changes in Oligomeric State. Results from Sanders and co-workers indicate that the folded protein is trimeric (C. Sanders, personal communication). If one of the denaturation phases corresponds to a change in oligomeric state, then a dependence on total protein concentration should be detectable. We found no change, however, in the unfolding transitions monitored by either UV or CD when protein concentration was varied over a 10-fold range (not shown). Other evidence suggests that the oligomer dissociates at low SDS concentrations and that the transition is invisible to our conformational probes. First of all, the protein migrates as a monomer on SDS−polyacrylamide gels, indicating that SDS does dissociate the trimer. Second, preliminary kinetic results show that the rate at which DGK activity is recovered from SDS-denatured protein is strongly concentration-dependent, indicating that the SDS-denatured protein is dissociated (not shown). Finally, if refolding is initiated from low denaturant concentrations, below the start of the first unfolding phase observed by CD, the concentration dependence of the refolding rate disappears. Thus, it appears that DGK dissociates prior to the first observed unfolding phase and that we are monitoring the unfolding of individual subunits.

Distinguishing between Unfolding of Membrane-Embedded and Cytoplasmic Domains. The changes in absorbance at 294 nm during SDS denaturation are the result of individual contributions of the four tryptophan residues in DGK. As shown in Figure 1, tryptophan residues are present in both the predicted transmembrane portion and the cytoplasmic portion of the protein. To ascertain which tryptophan residues and, thereby, which part of the protein accounts for the different phases observed during unfolding, a set of mutant proteins were prepared in which the Trp residues were replaced with different side chains. Four single mutants (W18L, W25L, W47F, and W112F) and a double mutant (W18L/W25L) were constructed. Both W25L and W112F could only be purified at low levels, were prone to aggregation, and either had low specific activities or lost activity rapidly upon purification. Consequently, we were unable to work with these proteins. W47F, W18L, and

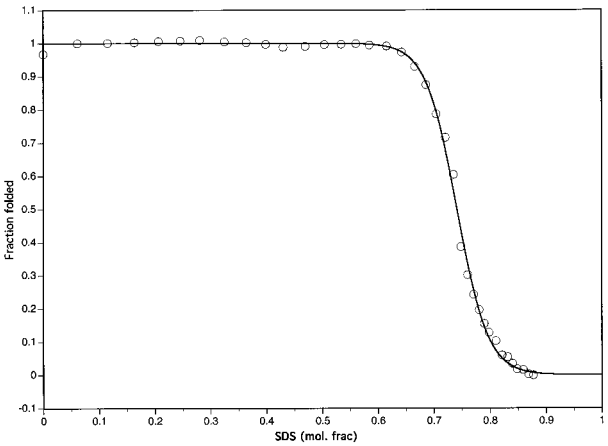

FIGURE 8: Unfolding of W18L/W25L. The mutant protein at 128 μM in 10 mM Pipes (pH 7.0), 0.30 M NaCl, and 1.0% DM was denatured by additions of 15% SDS in 10 mM Pipes and 0.30 M NaCl at pH 7.0. The data were baseline corrected as described in Materials and Methods. The curve is a fit to a two-state model as described in the text.

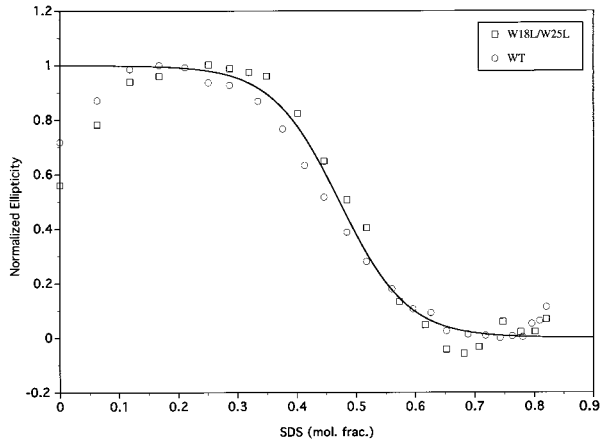

FIGURE 9: Denaturation of WT and W18L/W25L by CD. W18L/W25L (6 μM) (□) and wild-type (○) DGK (7 μM) in 1.0% DM, 10 mM Pipes, and 0.30 M NaCl at pH 7.0 were denatured by addition of aliquots of 15% SDS (w/v) in 10 mM Pipes and 0.30 M NaCl at pH 7.0. Ellipticity was monitored at 222 nm. Data points represent the average measurement within a 30 s time interval. The ellipticity values were normalized to range from 0 to 1 as described in Materials and Methods.

W18L/W25L, however, could be easily purified and had specific activities identical to that of the wild-type protein.

The UV unfolding curve for the W18L/W25L protein was significantly different than the unfolding curve for the wild-type protein. As shown in Figure 8, the initial enhancement and first denaturation phases observed for the wild-type protein have been virtually eliminated in the W18L/W25L mutant and the resulting denaturation curve contains only one major transition. The single transition observed for the W18L/W25L mutant protein corresponds to the second unfolding phase observed for the wild-type protein (Figure 5). In contrast, the unfolding of the W18L/W25L mutant monitored by ellipticity at 222 nm was identical to that of the wild-type protein (Figure 9). This indicates that the conformational changes occurring at low SDS concentrations are still present in the W18L/W25L protein. Because the tryptophan residues responsible for reporting these conformational changes in the wild-type protein are absent in W18L/W25L, however, these events become undetectable by the UV absorbance measurements.

Denaturation curves for W18L and W47F were indistinguishable from that of the wild-type protein. Thus, by process of elimination, we conclude that the first unfolding event involves W25 and the second unfolding event involves W112. Because the W25L and W112F mutants were ill-behaved, we were unable to verify this directly, however. Nevertheless, the poor stability of the purified W25L and W112F mutants is consistent with the idea that these side chains are buried in stabilizing interactions. Taken together, the results indicate that the first phase in the denaturation curves corresponds to an unfolding event involving the cytoplasmic domain, and the second phase corresponds to an unfolding event involving the membrane-embedded portion of the protein.

DISCUSSION

The results presented in this paper lead to the following model for the unfolding of the DGK subunits:

$$\mathrm{N} \underset{\Delta G_{u1}}{\overset{K_1}{\rightleftharpoons}} \mathrm{I} \underset{\Delta G_{u2}}{\overset{K_2}{\rightleftharpoons}} \mathrm{U} \qquad (2)$$

where N refers to the folded subunit, I refers to a partially folded intermediate, and U refers to the fully denatured protein. At low denaturant concentrations, N unfolds to the intermediate I. The early unfolding event involves Trp 25 in the cytoplasmic domain and results in a 15% drop in the helical content of the protein. In the second phase, an unfolding event occurs that involves part or all of the membrane-embedded portion of the protein and is reported by Trp 112. The second phase results in essentially no further reduction in helical content. The results suggest that the membrane-embedded portion of DGK is significantly more stable than the extramembrane portion.

Until we understand more about the denaturation of DGK in this system, and membrane proteins in general, quantitative interpretation of the results must be treated with appropriate skepticism. Nevertheless, we do have a system where equilibrium measurements can be made, so we felt it was worth attempting to describe the system with a simple quantitative model. We were, in fact, able to obtain good fits to the unfolding data using the simplest possible model, which assumes (1) that each unfolding phase represents a two-state, cooperative transition and (2) that there is a linear relationship between the unfolding free energy and the SDS concentration according to

$$\Delta G_u(X_{SDS}) = \Delta G_u(0) + mX_{SDS} \qquad (3)$$

where $\Delta G_u(X_{SDS})$ is the unfolding free energy at a particular concentration of SDS, $\Delta G_u(0)$ is the unfolding free energy in the absence of denaturant, m is a constant, and X_{SDS} is the mole fraction of SDS. The only free parameters are $\Delta G_u(0)$ and m. The first transition is most clearly monitored by the CD denaturation curves and the second transition by the UV denaturation curve for the W18L/W25L protein in which the first phase is transparent. Because the first transition is essentially complete by the start of the second transition (compare Figures 7 and 8), we can treat the two phases separately. Using the above assumptions, the best fits of the denaturation curves are shown in Figures 7 and 8. On the basis of the good fits obtained, it appears that the simple model describes the system very well. Although a

more complex denaturant binding model could be used to fit the data (Tanford, 1968, 1970; Pace & Vanderburg, 1979), it appears unwarranted at this point.[2] The estimated unfolding free energies in the absence of denaturant are 6 kcal/mol for ΔG_{u1} ($m = -12$ kcal/mol) and 16 kcal/mol for ΔG_{u2} ($m = -22$kcal/mol). Thus, the membrane-embedded structure in DM micelles is predicted to be extremely stable. Moreover, as the protein sequence is designed to stabilize the structure in the bilayer and not micelles, the stability in a bilayer may be even higher than what is observed in our system.

It is striking that the unfolding of other membrane protein systems is also consistent with early unfolding of the extramembrane domain. It has been demonstrated using GuHCl as a denaturant that the anion transporter, band 3 from human erythrocytes, exhibits biphasic behavior during denaturation (Oikawa et al., 1985). Oikawa and co-workers reported that the cytoplasmic domains of band 3 denatured at GuHCl concentrations similar to those of water-soluble proteins while the membrane-embedded portions were highly resistant to the effects of denaturant. Furthermore, Haltia and Friere have analyzed the results of thermal unfolding studies for a number of membrane proteins and suggest that most of the excess heat capacity observed in the unfolding of membrane proteins could be attributable to unfolding of the extramembrane domains only (Haltia & Freire, 1995). Moreover, where unfolding events can be assigned to particular subunits of membrane protein complexes, unfolding of the soluble subunits occurs at a lower temperature than that of the membrane-embedded portions. In short, our results with DGK are consistent with an overall picture indicating that the transmembrane domain portion of membrane proteins is usually much more stable than the extramembrane domains.

The high apparent stability of the membrane-embedded portions of membrane proteins is not surprising. Given the high stability of transmembrane helices, the unfolded state of a membrane protein would be expected to retain much of its native secondary structure (Engelman et al., 1986; Popot & Engelman, 1990; Zhang et al., 1992; Deber et al., 1993). Moreover, topological constraints in the membrane will impose additional order on the unfolded state. For soluble proteins, the conformational entropy cost associated with folding is huge and is the primary barrier to folding (Dill, 1990). In contrast, the entropy cost for folding membrane proteins should be relatively modest. As a result, achieving a highly stable membrane protein structure would require much less work in the form of stabilizing interactions than would be needed for soluble proteins.

From the extensive mutagenesis study of the DGK gene performed earlier in our laboratory, we were struck by the high level of tolerance found in the transmembrane domains (Wen et al., 1996). The vast majority of residues in the transmembrane domains could tolerate significant variation in size and shape. Indeed, the only transmembrane domain residue that appeared invariant in the Wen et al. study, Ile 59, has subsequently been shown to tolerate dramatically different side chains (unpublished). Two possible explanations for this tolerance were proposed. (1) The transmembrane domains are passive in the sense that their structure is not determined by specific interactions between side chains. or (2) the structure is overdetermined so that no one interaction is critical. The results in this paper favor the latter explanation. If the folded state of the membrane-embedded portion of DGK is more stable than the unfolded state by 16 kcal/mol as suggested by our data, it would be hard to find any single interaction that would destabilize the protein sufficiently to be detectable.

[2] When the data are fit to a denaturant binding model, the unfolding free energies are higher by less than 10%.

ACKNOWLEDGMENT

We thank Perlaminda Vida for help in preparing the W47 and W112 mutants, Charles Sanders for sharing the colorimetric assay with us prior to publication and for many helpful discussions, Juan Wen, Yufeng Zhou, and Cindy Chen for much technical advice, and Todd Yeates and Tau-Mu Yi for thoughtful reading of a preliminary version of the manuscript.

REFERENCES

Arrondo, J., Castresana, J., Valpuesta, J., & Goni, F. (1994) *Biochemistry 33*, 11650−11655.
Bohnenberger, E., & Sandermann, H. (1979) *Eur. J. Biochem. 94*, 401−407.
Booth, P., Flitsch, S., Stern, L., Greenhalgh, D., Kim, P., & Khorana, H. (1995) *Nat. Struct. Biol. 2*, 139−143.
Brouillette, C., Muccio, D., & Finney, T. (1987) *Biochemistry 26*, 7431.
Brouillette, C., McMichens, R., Stern, L., & Khorana, H. (1989) *Proteins: Struct., Funct., Genet. 5*, 38.
Copeland, R. A. (1994) *Methods for Protein Analysis*, Chapman & Hall, New York and London.
Cramer, W. A., Whitmarsh, J., & Low, P. S. (1981) *Biochemistry 20*, 157−162.
Davio, S., & Low, P. (1982) *Biochemistry 21*, 3585−3593.
Deber, C. M., Khan, A. R., Li, Z., Joensson, C., Glibowicka, M., & Wang, J. (1993) *Proc. Natl. Acad. Sci. U.S.A. 90*, 11648−11652.
Dill, K. (1990) *Biochemistry 29*, 7133−7155.
Dornmair, K., Kiefer, H., & Jahnig, F. (1990) *J. Biol. Chem. 265*, 18907−18911.
Dubois, M., Gelles, K. A., Hamilton, J. K., Rebers, P. A., & Smith, F. (1956) *Anal. Chem. 28*, 350−356.
Eisle, J.-L., & Rosenbusch, J. (1990) *J. Biol. Chem. 265*, 10217−10220.
Engelman, D. M., Steitz, T. A., & Goldman, A. (1986) *Annu. Rev. Biophys. Biophys. Chem. 15*, 321−353.
Haltia, T., & Freire, E. (1995) *Biochim. Biophys. Acta 1228*, 1−27.
He, B., Zhang, Y., Zhang, T., Wang, H. R., & Zhou, H. M. (1995) *J. Protein Chem. 14*, 349−357.
Hill, B., Cook, K., & Robinson, N. (1988) *Biochemistry 27*, 4741−4747.
Huang, K.-S., Bayley, J., Liao, M., London, E., & Khorana, H. (1981) *J. Biol. Chem. 256*, 3802−3809.
Kahn, T., Sturtevant, J., & Engelman, D. (1992) *Biochemistry 31*, 8829.
Klug, C., Su, W., Liu, J., Klebba, P., & Feix, J. (1995) *Biochemistry 34*, 14230−14236.
Lightner, V., Bell, R., & Modrich, P. (1983) *J. Biol. Chem. 258*, 10856.
London, E., & Khorana, H. (1982) *J. Biol. Chem. 257*, 7003−7011.
Loomis, C., Walsh, J., & Bell, R. (1985) *J. Biol. Chem. 260*, 4091.
Manavalan, P., & Johnson, W. (1987) *Anal. Biochem. 167*, 76−85.
Maneri, L., & Low, P. (1988) *J. Biol. Chem. 263*, 16170−16178.
Mattice, W., Riser, J., & Clark, D. (1976) *Biochemistry 15*, 4264−4272.
Miller, K., McKinstry, M., Hunt, W., & Nixon, B. (1992) *Mol. Plant-Microbe Interact. 5*, 363−371.
Morin, P., Diggs, D., & Freire, E. (1990) *Biochemistry 29*, 781−788.

Oikawa, K., Lieberman, D. M., & Reithmeier, R. A. (1985) *Biochemistry 24*, 2843−2848.
Pace, C. N., & Vanderburg, K. E. (1979) *Biochemistry 18*, 288−292.
Popot, J., & Engelman, D. (1990) *Biochemistry 29*, 4031−4037.
Rao, K. S., & Prakash, V. (1993) *J. Biol. Chem. 268*, 14769−14775.
Reynolds, J., & Tanford, C. (1970) *J. Biol. Chem. 245*, 5161−5165.
Rigell, C., de Saussure, C., & Freire, E. (1985) *Biochemistry 24*, 5638.
Sanders, C., Czerski, L., Vinogradova, O., Badola, P., Song, D., & Smith, S. (1996) *Biochemistry 35*, 8610−8618.
Smith, R., O'Toole, J., Maguire, M., & Sanders, C. (1994) *J. Bacteriol. 176*, 5459−5465.
Tanford, C. (1968) *Adv. Protein Chem. 23*, 121−282.
Tanford, C. (1970) *Adv. Protein Chem. 24*, 1−95.
Thompson, L. K., Sturtevant, J. M., & Brudvig, G. W. (1986) *Biochemistry 25*, 6161−6169.
Thompson, L. K., Blaylock, R., Sturtevant, J. M., & Brudvig, G. W. (1989) *Biochemistry 28*, 6686−6695.
Walsh, J., & Bell, R. (1986a) *J. Biol. Chem. 261*, 6239.
Walsh, J., & Bell, R. (1986b) *J. Biol. Chem. 261*, 15062.
Walsh, J., Fahrner, L., & Bell, R. (1990) *J. Biol. Chem. 265*, 4374.
Wen, J., Chen, X., & Bowie, J. (1996) *Nat. Struct. Biol. 3*, 141−148.
Yang, J. T., Wu, C., & Martinez, H. (1986) *Methods Enzymol. 130*, 208−269.
Zhang, Y. P., Lewis, R. N., Hodges, R. S., & McElhaney, R. N. (1992) *Biochemistry 31*, 11579−11588.

BI963095J